Evaluating pseudorange multipath effects at stations in the National CORS Network

Stephen Hilla · Michael Cline

Abstract A preliminary study was conducted to evaluate the amount of pseudorange multipath at 390+ sites in the National Continuously Operating Reference Station (CORS) Network. The National CORS Network is a cooperative effort involving over 110 different agencies, universities, and private companies who seek to make GPS data from dual-frequency receivers located throughout the United States and its territories available to the general public. For CORS users, pseudorange multipath can seriously degrade the accuracy of any application that relies on precise measurements of the pseudorange observable over a short period of time, including differential pseudorange navigation, kinematic and rapid-static surveying, and ionospheric monitoring. The main objectives of this study were to identify the most affected and least affected sites in the network, to closely investigate problematic sites, and to compare various receiver/antenna combinations. Dual-frequency carrier phase and pseudorange measurements were used to estimate the amount of L1 and L2 pseudorange multipath at each site over a one-year period. Some of the most severely affected sites were maritime Differential GPS and Nationwide Differential GPS (DGPS/NDGPS) sites. Photographs obtained for these sites verified the presence of transmission towers and other reflectors in close proximity to the GPS antennas. Plotting the variations of the L1 and L2 pseudorange multipath with respect to azimuth and elevation further verified that even above a 60° elevation angle there was still as much as five meters of pseudorange multipath at some sites. The least affected sites were the state networks installed in Ohio and Michigan; these sites used excellent antenna mounts, choke ring antennas, and new receiver technology. A comparison of the 12 most commonly used receiver/antenna combinations in the CORS Network indicated that newer receivers such as the Ashtech UZ-12, Leica RS-500, and Trimble 5700 help to significantly mitigate pseudorange multipath, while the receivers/antennas at some DGPS/NDGPS sites, and the antennas formerly used at the Wide Area Augmentation System (WAAS) sites, are among those most affected by pseudorange multipath. The receiver/antenna comparison did not take into account the potential presence of reflectors at the sites (i.e., it is possible that a well-performing receiver/antenna combination could have been consistently placed at very poor site locations, and vice-versa).

Introduction

An initial study has been done to estimate the amount of pseudorange multipath at 390+ sites in the National CORS Network. The study was conducted to identify the most affected and least affected sites in the network, to compare different receiver/antenna combinations, and to investigate closely those sites that appear to be severely affected by multipath. Identification of severely affected sites will help with other research at the National Geodetic Survey (NGS) such as ionospheric studies (mapping Total Electron Content), studies related to the High Accuracy National Differential Global Positioning System (HA-NDGPS) demonstration project, and studies done to evaluate methods and equipment for the in-situ calibration of carrier phase multipath (e.g., Brown and Wang 1999). Comparing different receiver/antenna combinations has highlighted the equipment and the antenna mounting techniques that seem to be working best in the current network. Closely investigating the most severely affected sites, both by examining photographs and by analyzing

Received: 20 August 2003 / Accepted: 27 September 2003
Published online: 27 November 2003

S. Hilla (✉) · M. Cline
National Geodetic Survey, NOAA, 1315 East-West Highway, Silver Spring, MD 20910, USA
E-mail: steve.hilla@noaa.gov
Tel.: +1-301-7132851
Fax: +1-301-7134475

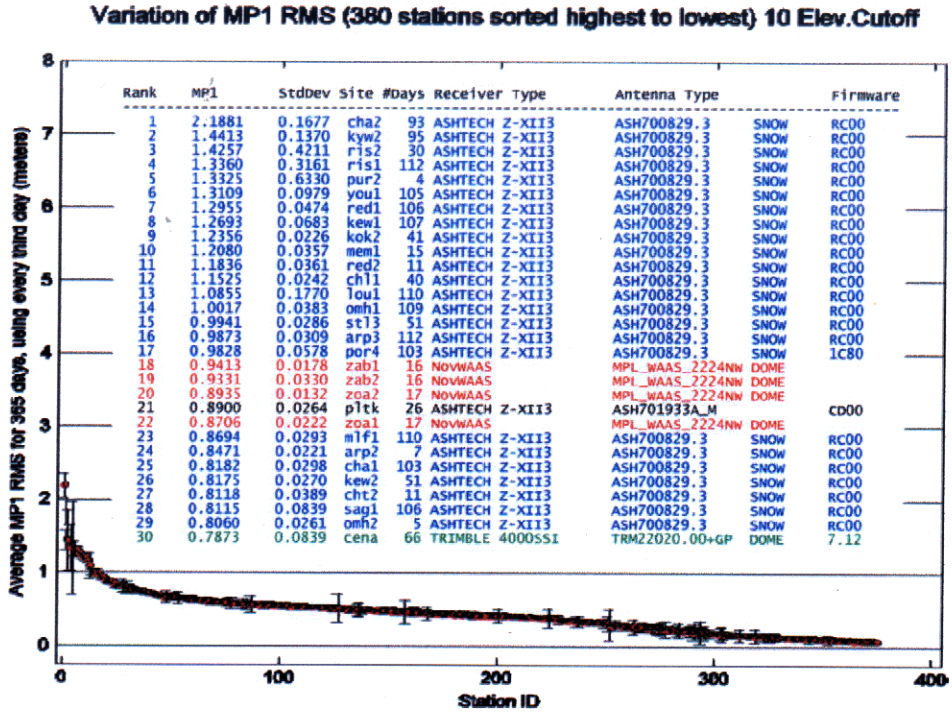

Rank	MP1	StdDev	Site	#Days	Receiver Type	Antenna Type		Firmware
1	2.1881	0.1677	cha2	93	ASHTECH Z-XII3	ASH700829.3	SNOW	RC00
2	1.4413	0.1370	kyw2	95	ASHTECH Z-XII3	ASH700829.3	SNOW	RC00
3	1.4257	0.4211	ris2	30	ASHTECH Z-XII3	ASH700829.3	SNOW	RC00
4	1.3360	0.3161	ris1	112	ASHTECH Z-XII3	ASH700829.3	SNOW	RC00
5	1.3325	0.6330	pur2	4	ASHTECH Z-XII3	ASH700829.3	SNOW	RC00
6	1.3109	0.0979	you1	105	ASHTECH Z-XII3	ASH700829.3	SNOW	RC00
7	1.2955	0.0474	red1	106	ASHTECH Z-XII3	ASH700829.3	SNOW	RC00
8	1.2693	0.0683	kew1	107	ASHTECH Z-XII3	ASH700829.3	SNOW	RC00
9	1.2356	0.0226	kok2	41	ASHTECH Z-XII3	ASH700829.3	SNOW	RC00
10	1.2080	0.0357	mem1	15	ASHTECH Z-XII3	ASH700829.3	SNOW	RC00
11	1.1836	0.0361	red2	11	ASHTECH Z-XII3	ASH700829.3	SNOW	RC00
12	1.1525	0.0242	chl1	40	ASHTECH Z-XII3	ASH700829.3	SNOW	RC00
13	1.0855	0.1770	lou1	110	ASHTECH Z-XII3	ASH700829.3	SNOW	RC00
14	1.0017	0.0383	omh1	109	ASHTECH Z-XII3	ASH700829.3	SNOW	RC00
15	0.9941	0.0286	stl3	51	ASHTECH Z-XII3	ASH700829.3	SNOW	RC00
16	0.9873	0.0309	arp3	112	ASHTECH Z-XII3	ASH700829.3	SNOW	RC00
17	0.9828	0.0578	por4	103	ASHTECH Z-XII3	ASH700829.3	SNOW	1C80
18	0.9413	0.0178	zab1	16	NovWAAS	MPL_WAAS_2224NW	DOME	
19	0.9331	0.0330	zab2	16	NovWAAS	MPL_WAAS_2224NW	DOME	
20	0.8935	0.0132	zoa2	17	NovWAAS	MPL_WAAS_2224NW	DOME	
21	0.8900	0.0264	pltk	26	ASHTECH Z-XII3	ASH701933A_M		CD00
22	0.8706	0.0222	zoa1	17	NovWAAS	MPL_WAAS_2224NW	DOME	
23	0.8694	0.0293	mlf1	110	ASHTECH Z-XII3	ASH700829.3	SNOW	RC00
24	0.8471	0.0221	arp2	7	ASHTECH Z-XII3	ASH700829.3	SNOW	RC00
25	0.8182	0.0298	cha1	103	ASHTECH Z-XII3	ASH700829.3	SNOW	RC00
26	0.8175	0.0270	kew2	51	ASHTECH Z-XII3	ASH700829.3	SNOW	RC00
27	0.8118	0.0389	cht2	11	ASHTECH Z-XII3	ASH700829.3	SNOW	RC00
28	0.8115	0.0839	sag1	106	ASHTECH Z-XII3	ASH700829.3	SNOW	RC00
29	0.8060	0.0261	omh2	5	ASHTECH Z-XII3	ASH700829.3	SNOW	RC00
30	0.7873	0.0839	cena	66	TRIMBLE 4000SSI	TRM22020.00+GP	DOME	7.12

Fig. 1
Average MP1 RMS values using 10° elevation mask. *Insert* shows the 30 most affected sites

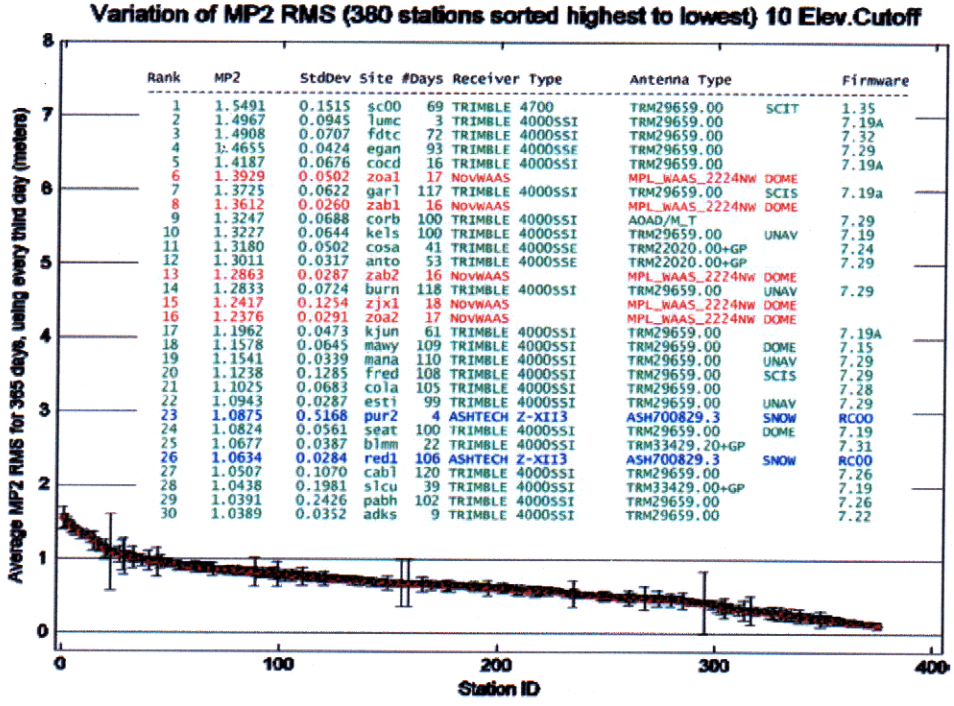

Rank	MP2	StdDev	Site	#Days	Receiver Type	Antenna Type		Firmware
1	1.5491	0.1515	sc00	69	TRIMBLE 4700	TRM29659.00	SCIT	1.35
2	1.4967	0.0945	lumc	3	TRIMBLE 4000SSI	TRM29659.00		7.19A
3	1.4908	0.0707	fdtc	72	TRIMBLE 4000SSI	TRM29659.00		7.32
4	1.4655	0.0424	egan	93	TRIMBLE 4000SSE	TRM29659.00		7.29
5	1.4187	0.0676	cocd	16	TRIMBLE 4000SSI	TRM29659.00		7.19A
6	1.3929	0.0502	zoa1	17	NovWAAS	MPL_WAAS_2224NW	DOME	
7	1.3725	0.0622	garl	117	TRIMBLE 4000SSI	TRM29659.00	SCIS	7.19a
8	1.3612	0.0260	zab1	16	NovWAAS	MPL_WAAS_2224NW	DOME	
9	1.3247	0.0688	corb	100	TRIMBLE 4000SSI	AOAD/M_T		7.29
10	1.3227	0.0644	kels	100	TRIMBLE 4000SSI	TRM29659.00	UNAV	7.19
11	1.3180	0.0502	cosa	41	TRIMBLE 4000SSE	TRM22020.00+GP		7.24
12	1.3011	0.0317	anto	53	TRIMBLE 4000SSE	TRM22020.00+GP		7.29
13	1.2863	0.0287	zab2	16	NovWAAS	MPL_WAAS_2224NW	DOME	
14	1.2833	0.0724	burn	118	TRIMBLE 4000SSI	TRM29659.00	UNAV	7.29
15	1.2417	0.1254	zjx1	18	NovWAAS	MPL_WAAS_2224NW	DOME	
16	1.2376	0.0291	zoa2	17	NovWAAS	MPL_WAAS_2224NW	DOME	
17	1.1962	0.0473	kjun	61	TRIMBLE 4000SSI	TRM29659.00		7.19A
18	1.1578	0.0645	mawy	109	TRIMBLE 4000SSI	TRM29659.00	DOME	7.15
19	1.1541	0.0339	mana	110	TRIMBLE 4000SSI	TRM29659.00	UNAV	7.29
20	1.1238	0.1285	fred	108	TRIMBLE 4000SSI	TRM29659.00	SCIS	7.29
21	1.1025	0.0683	cola	105	TRIMBLE 4000SSI	TRM29659.00		7.28
22	1.0943	0.0287	esti	99	TRIMBLE 4000SSI	TRM29659.00	UNAV	7.29
23	1.0875	0.5168	pur2	4	ASHTECH Z-XII3	ASH700829.3	SNOW	RC00
24	1.0824	0.0561	seat	100	TRIMBLE 4000SSI	TRM29659.00	DOME	7.19
25	1.0677	0.0387	blmm	22	TRIMBLE 4000SSI	TRM33429.20+GP		7.31
26	1.0634	0.0284	red1	106	ASHTECH Z-XII3	ASH700829.3	SNOW	RC00
27	1.0507	0.1070	cabl	120	TRIMBLE 4000SSI	TRM29659.00		7.26
28	1.0438	0.1981	slcu	39	TRIMBLE 4000SSI	TRM33429.00+GP		7.19
29	1.0391	0.2426	pabh	102	TRIMBLE 4000SSI	TRM29659.00		7.26
30	1.0389	0.0352	adks	9	TRIMBLE 4000SSI	TRM29659.00		7.22

Fig. 2
Average MP2 RMS values using 10° elevation mask. *Insert* shows the 30 most affected sites

multipath variations with respect to elevation angle and azimuth, has helped lead to a better understanding of the kinds of factors contributing to pseudorange multipath at a site.

Our main tool for calculating the variation of the L1 and L2 pseudorange multipath at each site was the TEQC software (Estey and Meertens 1999). It computes the MP1 and MP2 linear combinations using both pseudorange and carrier phase data to eliminate the effects of station

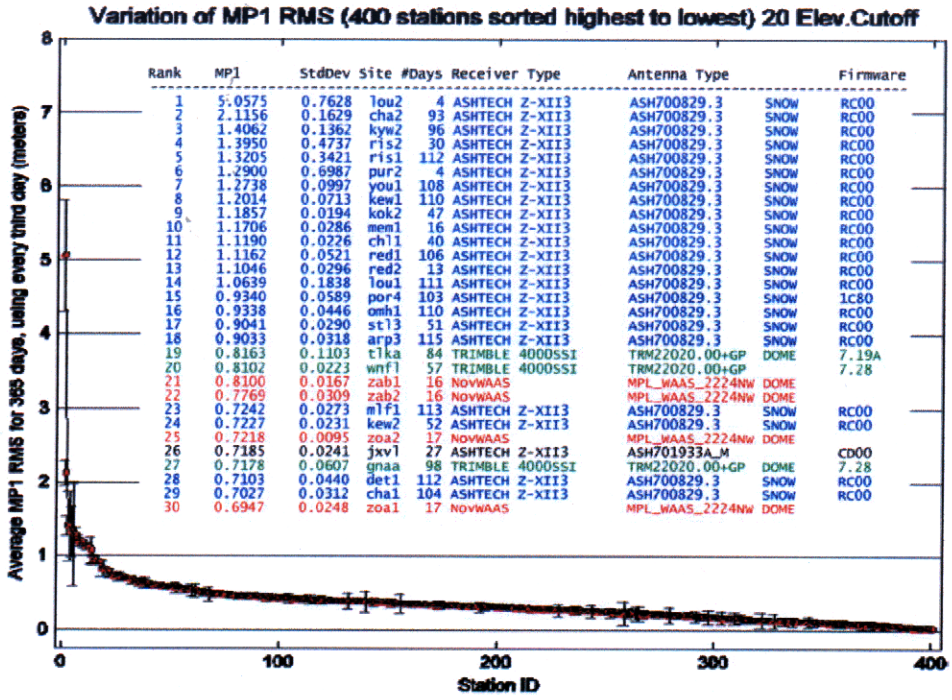

Rank	MP1	StdDev	Site	#Days	Receiver Type	Antenna Type		Firmware
1	5.0575	0.7628	lou2	4	ASHTECH Z-XII3	ASH700829.3	SNOW	RC00
2	2.1156	0.1629	cha2	93	ASHTECH Z-XII3	ASH700829.3	SNOW	RC00
3	1.4062	0.1362	kyw2	96	ASHTECH Z-XII3	ASH700829.3	SNOW	RC00
4	1.3950	0.4737	ris2	30	ASHTECH Z-XII3	ASH700829.3	SNOW	RC00
5	1.3205	0.3421	ris1	112	ASHTECH Z-XII3	ASH700829.3	SNOW	RC00
6	1.2900	0.6987	pur2	4	ASHTECH Z-XII3	ASH700829.3	SNOW	RC00
7	1.2738	0.0997	you1	108	ASHTECH Z-XII3	ASH700829.3	SNOW	RC00
8	1.2014	0.0713	kew1	110	ASHTECH Z-XII3	ASH700829.3	SNOW	RC00
9	1.1857	0.0194	kok2	47	ASHTECH Z-XII3	ASH700829.3	SNOW	RC00
10	1.1706	0.0286	mem1	16	ASHTECH Z-XII3	ASH700829.3	SNOW	RC00
11	1.1190	0.0226	chl1	40	ASHTECH Z-XII3	ASH700829.3	SNOW	RC00
12	1.1162	0.0521	red1	106	ASHTECH Z-XII3	ASH700829.3	SNOW	RC00
13	1.1046	0.0296	red2	13	ASHTECH Z-XII3	ASH700829.3	SNOW	RC00
14	1.0639	0.1838	lou1	111	ASHTECH Z-XII3	ASH700829.3	SNOW	RC00
15	0.9340	0.0589	por4	103	ASHTECH Z-XII3	ASH700829.3	SNOW	1C80
16	0.9338	0.0446	omh1	110	ASHTECH Z-XII3	ASH700829.3	SNOW	RC00
17	0.9041	0.0290	stl3	51	ASHTECH Z-XII3	ASH700829.3	SNOW	RC00
18	0.9033	0.0318	arp3	115	ASHTECH Z-XII3	ASH700829.3	SNOW	RC00
19	0.8163	0.1103	tlka	84	TRIMBLE 4000SSI	TRM22020.00+GP	DOME	7.19A
20	0.8102	0.0223	wnfl	57	TRIMBLE 4000SSI	TRM22020.00+GP		7.28
21	0.8100	0.0167	zab1	16	NovWAAS	MPL_WAAS_2224NW	DOME	
22	0.7769	0.0309	zab2	16	NovWAAS	MPL_WAAS_2224NW	DOME	
23	0.7242	0.0273	mlf1	113	ASHTECH Z-XII3	ASH700829.3	SNOW	RC00
24	0.7227	0.0231	kew2	52	ASHTECH Z-XII3	ASH700829.3	SNOW	RC00
25	0.7218	0.0095	zoa2	17	NovWAAS	MPL_WAAS_2224NW	DOME	
26	0.7185	0.0241	jxvl	27	ASHTECH Z-XII3	ASH701933A_M		CD00
27	0.7178	0.0607	gnaa	98	TRIMBLE 4000SSI	TRM22020.00+GP	DOME	7.28
28	0.7103	0.0440	det1	112	ASHTECH Z-XII3	ASH700829.3	SNOW	RC00
29	0.7027	0.0312	cha1	104	ASHTECH Z-XII3	ASH700829.3	SNOW	RC00
30	0.6947	0.0248	zoa1	17	NovWAAS	MPL_WAAS_2224NW	DOME	

Fig. 3
Average MP1 RMS values using 20° elevation mask. *Insert* shows the 30 most affected sites

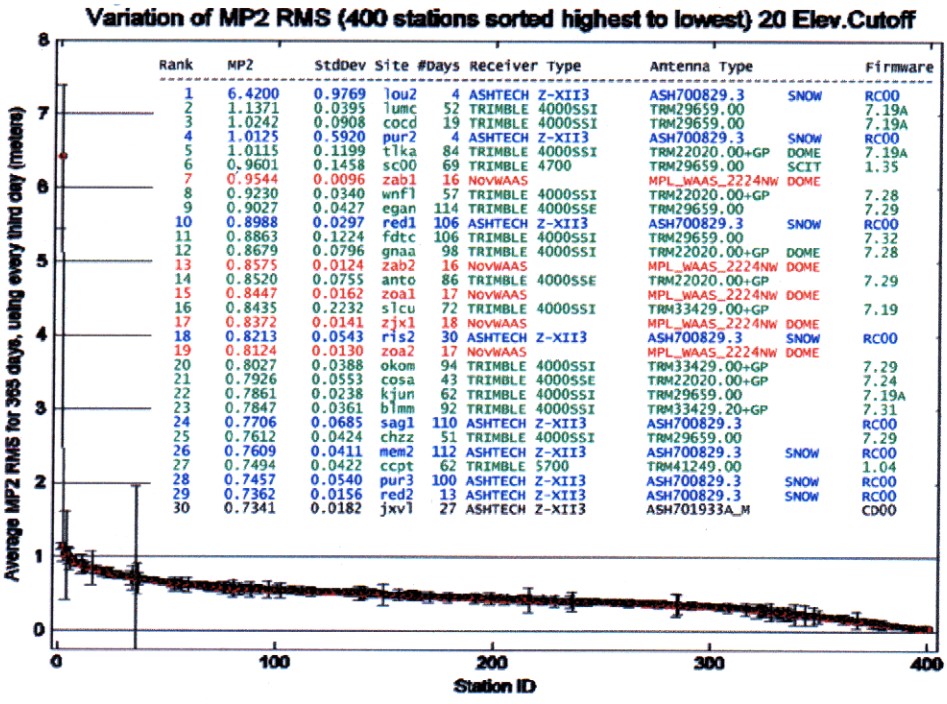

Rank	MP2	StdDev	Site	#Days	Receiver Type	Antenna Type		Firmware
1	6.4200	0.9769	lou2	4	ASHTECH Z-XII3	ASH700829.3	SNOW	RC00
2	1.1371	0.0395	lumc	52	TRIMBLE 4000SSI	TRM29659.00		7.19A
3	1.0242	0.0908	cocd	19	TRIMBLE 4000SSI	TRM29659.00		7.19A
4	1.0125	0.5920	pur2	4	ASHTECH Z-XII3	ASH700829.3	SNOW	RC00
5	1.0115	0.1199	tlka	84	TRIMBLE 4000SSI	TRM22020.00+GP	DOME	7.19A
6	0.9601	0.1458	sc00	69	TRIMBLE 4700	TRM29659.00	SCIT	1.35
7	0.9544	0.0096	zab1	16	NovWAAS	MPL_WAAS_2224NW	DOME	
8	0.9230	0.0340	wnfl	57	TRIMBLE 4000SSI	TRM22020.00+GP		7.28
9	0.9027	0.0427	egan	114	TRIMBLE 4000SSE	TRM29659.00		7.29
10	0.8988	0.0297	red1	106	ASHTECH Z-XII3	ASH700829.3	SNOW	RC00
11	0.8863	0.1224	fdtc	106	TRIMBLE 4000SSI	TRM29659.00		7.32
12	0.8679	0.0796	gnaa	98	TRIMBLE 4000SSI	TRM22020.00+GP	DOME	7.28
13	0.8575	0.0124	zab2	16	NovWAAS	MPL_WAAS_2224NW	DOME	
14	0.8520	0.0755	anto	86	TRIMBLE 4000SSE	TRM22020.00+GP		7.29
15	0.8447	0.0162	zoa1	17	NovWAAS	MPL_WAAS_2224NW	DOME	
16	0.8435	0.2232	slcu	72	TRIMBLE 4000SSI	TRM33429.00+GP		7.19
17	0.8372	0.0141	zjx1	18	NovWAAS	MPL_WAAS_2224NW	DOME	
18	0.8213	0.0543	ris2	30	ASHTECH Z-XII3	ASH700829.3	SNOW	RC00
19	0.8124	0.0130	zoa2	17	NovWAAS	MPL_WAAS_2224NW	DOME	
20	0.8027	0.0388	okom	94	TRIMBLE 4000SSI	TRM33429.00+GP		7.29
21	0.7926	0.0553	cosa	43	TRIMBLE 4000SSE	TRM22020.00+GP		7.24
22	0.7861	0.0238	kjun	62	TRIMBLE 4000SSI	TRM29659.00		7.19A
23	0.7847	0.0361	blmm	92	TRIMBLE 4000SSI	TRM33429.20+GP		7.31
24	0.7706	0.0685	sag1	110	ASHTECH Z-XII3	ASH700829.3		RC00
25	0.7612	0.0424	chzz	51	TRIMBLE 4000SSI	TRM29659.00		7.29
26	0.7609	0.0411	mem2	112	ASHTECH Z-XII3	ASH700829.3	SNOW	RC00
27	0.7494	0.0422	ccpt	62	TRIMBLE 5700	TRM41249.00		1.04
28	0.7457	0.0540	pur3	100	ASHTECH Z-XII3	ASH700829.3	SNOW	RC00
29	0.7362	0.0156	red2	13	ASHTECH Z-XII3	ASH700829.3	SNOW	RC00
30	0.7341	0.0182	jxvl	27	ASHTECH Z-XII3	ASH701933A_M		CD00

Fig. 4
Average MP2 RMS values using 20° elevation mask. *Insert* shows the 30 most affected sites

clocks, satellite clocks, tropospheric delay, and ionospheric delay:

$$MP1 \equiv P_1 - \left(1+\frac{2}{\alpha-1}\right)L_1 + \left(\frac{2}{\alpha-1}\right)L_2$$
$$= M_1 + B_1 - \left(1+\frac{2}{\alpha-1}\right)m_1 + \left(\frac{2}{\alpha-1}\right)m_2 \qquad (1)$$

where $B_1 \equiv -\left(1+\frac{2}{\alpha-1}\right)n_1\lambda_1 + \left(\frac{2}{\alpha-1}\right)n_2\lambda_2$, and $\alpha = \frac{f_1^2}{f_2^2}$

$$MP2 \equiv P_2 - \left(\frac{2\alpha}{\alpha-1}\right)L_1 + \left(\frac{2\alpha}{\alpha-1}-1\right)L_2$$
$$= M_2 + B_2 - \left(\frac{2\alpha}{\alpha-1}\right)m_1 + \left(\frac{2\alpha}{\alpha-1}-1\right)m_2 \qquad (2)$$

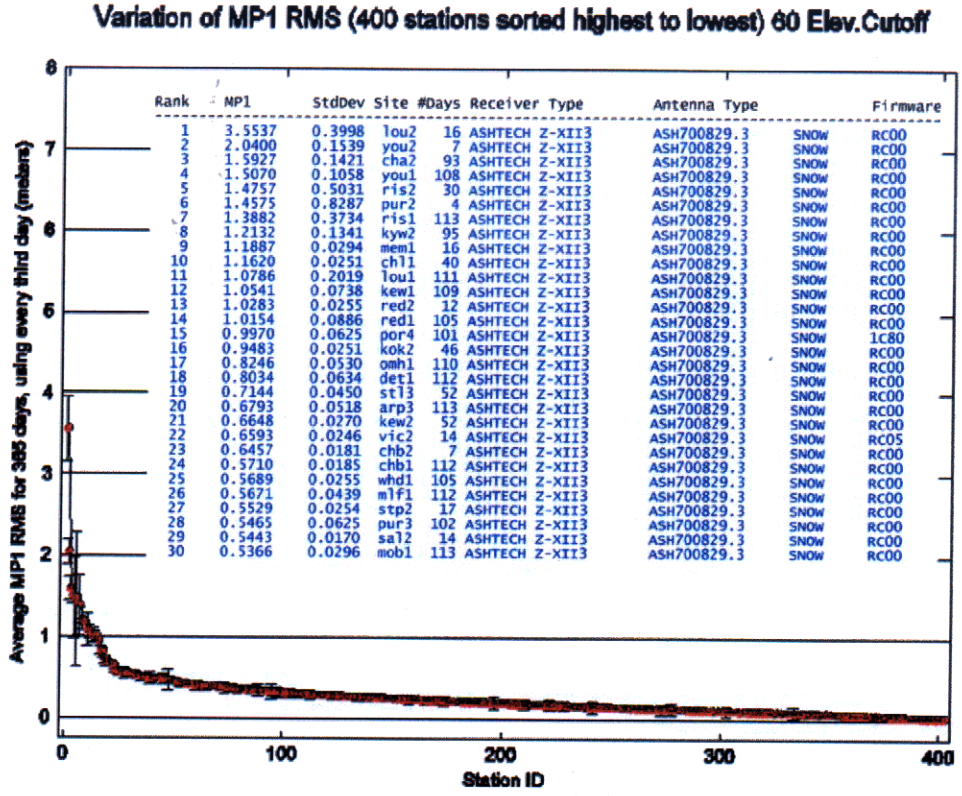

Rank	MP1	StdDev	Site	#Days	Receiver Type	Antenna Type		Firmware
1	3.5537	0.3998	lou2	16	ASHTECH Z-XII3	ASH700829.3	SNOW	RC00
2	2.0400	0.1539	you2	7	ASHTECH Z-XII3	ASH700829.3	SNOW	RC00
3	1.5927	0.1421	cha2	93	ASHTECH Z-XII3	ASH700829.3	SNOW	RC00
4	1.5070	0.1058	you1	108	ASHTECH Z-XII3	ASH700829.3	SNOW	RC00
5	1.4757	0.5031	ris2	30	ASHTECH Z-XII3	ASH700829.3	SNOW	RC00
6	1.4575	0.8287	pur2	4	ASHTECH Z-XII3	ASH700829.3	SNOW	RC00
7	1.3882	0.3734	ris1	113	ASHTECH Z-XII3	ASH700829.3	SNOW	RC00
8	1.2132	0.1341	kyw2	95	ASHTECH Z-XII3	ASH700829.3	SNOW	RC00
9	1.1887	0.0294	mem1	16	ASHTECH Z-XII3	ASH700829.3	SNOW	RC00
10	1.1620	0.0251	ch11	40	ASHTECH Z-XII3	ASH700829.3	SNOW	RC00
11	1.0786	0.2019	lou1	111	ASHTECH Z-XII3	ASH700829.3	SNOW	RC00
12	1.0541	0.0738	kew1	109	ASHTECH Z-XII3	ASH700829.3	SNOW	RC00
13	1.0283	0.0255	red2	12	ASHTECH Z-XII3	ASH700829.3	SNOW	RC00
14	1.0154	0.0886	red1	105	ASHTECH Z-XII3	ASH700829.3	SNOW	RC00
15	0.9970	0.0625	por4	101	ASHTECH Z-XII3	ASH700829.3	SNOW	1C80
16	0.9483	0.0251	kok2	46	ASHTECH Z-XII3	ASH700829.3	SNOW	RC00
17	0.8246	0.0530	omh1	110	ASHTECH Z-XII3	ASH700829.3	SNOW	RC00
18	0.8034	0.0634	det1	112	ASHTECH Z-XII3	ASH700829.3	SNOW	RC00
19	0.7144	0.0450	stl3	52	ASHTECH Z-XII3	ASH700829.3	SNOW	RC00
20	0.6793	0.0518	arp3	113	ASHTECH Z-XII3	ASH700829.3	SNOW	RC00
21	0.6648	0.0270	kew2	52	ASHTECH Z-XII3	ASH700829.3	SNOW	RC00
22	0.6593	0.0246	vic2	14	ASHTECH Z-XII3	ASH700829.3	SNOW	RC05
23	0.6457	0.0181	chb2	7	ASHTECH Z-XII3	ASH700829.3	SNOW	RC00
24	0.5710	0.0185	chb1	112	ASHTECH Z-XII3	ASH700829.3	SNOW	RC00
25	0.5689	0.0255	whd1	105	ASHTECH Z-XII3	ASH700829.3	SNOW	RC00
26	0.5671	0.0439	mlf1	112	ASHTECH Z-XII3	ASH700829.3	SNOW	RC00
27	0.5529	0.0254	stp2	17	ASHTECH Z-XII3	ASH700829.3	SNOW	RC00
28	0.5465	0.0625	pur3	102	ASHTECH Z-XII3	ASH700829.3	SNOW	RC00
29	0.5443	0.0170	sal2	14	ASHTECH Z-XII3	ASH700829.3	SNOW	RC00
30	0.5366	0.0296	mob1	113	ASHTECH Z-XII3	ASH700829.3	SNOW	RC00

Fig. 5
Average MP1 RMS values using 60° elevation mask. *Insert* shows the 30 most affected sites

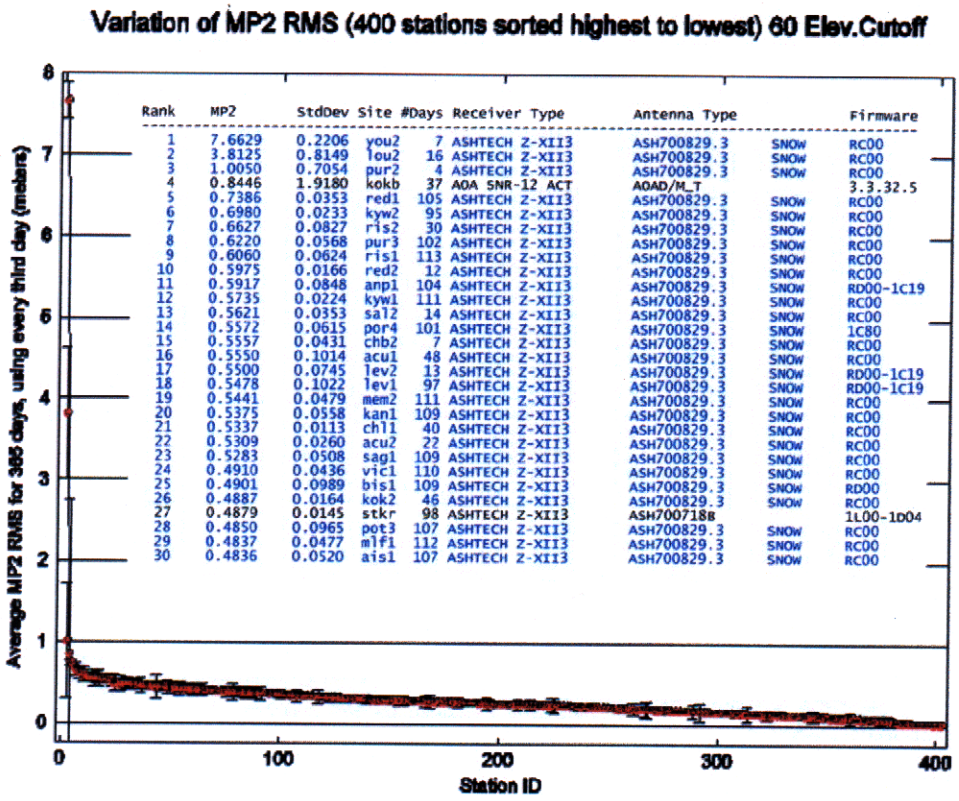

Rank	MP2	StdDev	Site	#Days	Receiver Type	Antenna Type		Firmware
1	7.6629	0.2206	you2	7	ASHTECH Z-XII3	ASH700829.3	SNOW	RC00
2	3.8125	0.8149	lou2	16	ASHTECH Z-XII3	ASH700829.3	SNOW	RC00
3	1.0050	0.7054	pur2	4	ASHTECH Z-XII3	ASH700829.3	SNOW	RC00
4	0.8446	1.9180	kokb	37	AOA SNR-12 ACT	AOAD/M_T		3.3.32.5
5	0.7386	0.0353	red1	105	ASHTECH Z-XII3	ASH700829.3	SNOW	RC00
6	0.6980	0.0233	kyw2	95	ASHTECH Z-XII3	ASH700829.3	SNOW	RC00
7	0.6627	0.0827	ris2	30	ASHTECH Z-XII3	ASH700829.3	SNOW	RC00
8	0.6220	0.0568	pur3	102	ASHTECH Z-XII3	ASH700829.3	SNOW	RC00
9	0.6060	0.0624	ris1	113	ASHTECH Z-XII3	ASH700829.3	SNOW	RC00
10	0.5975	0.0166	red2	12	ASHTECH Z-XII3	ASH700829.3	SNOW	RC00
11	0.5917	0.0848	anp1	104	ASHTECH Z-XII3	ASH700829.3	SNOW	RD00-1C19
12	0.5735	0.0224	kyw1	111	ASHTECH Z-XII3	ASH700829.3	SNOW	RC00
13	0.5621	0.0353	sal2	14	ASHTECH Z-XII3	ASH700829.3	SNOW	RC00
14	0.5572	0.0615	por4	101	ASHTECH Z-XII3	ASH700829.3	SNOW	1C80
15	0.5557	0.0431	chb2	7	ASHTECH Z-XII3	ASH700829.3	SNOW	RC00
16	0.5550	0.1014	acu1	48	ASHTECH Z-XII3	ASH700829.3	SNOW	RC00
17	0.5500	0.0745	lev2	13	ASHTECH Z-XII3	ASH700829.3	SNOW	RD00-1C19
18	0.5478	0.1022	lev1	97	ASHTECH Z-XII3	ASH700829.3	SNOW	RD00-1C19
19	0.5441	0.0479	mem2	111	ASHTECH Z-XII3	ASH700829.3	SNOW	RC00
20	0.5375	0.0558	kan1	109	ASHTECH Z-XII3	ASH700829.3	SNOW	RC00
21	0.5337	0.0113	ch11	40	ASHTECH Z-XII3	ASH700829.3	SNOW	RC00
22	0.5309	0.0260	acu2	22	ASHTECH Z-XII3	ASH700829.3	SNOW	RC00
23	0.5283	0.0508	sag1	109	ASHTECH Z-XII3	ASH700829.3	SNOW	RC00
24	0.4910	0.0436	vic1	110	ASHTECH Z-XII3	ASH700829.3	SNOW	RC00
25	0.4901	0.0989	bis1	109	ASHTECH Z-XII3	ASH700829.3	SNOW	RD00
26	0.4887	0.0164	kok2	46	ASHTECH Z-XII3	ASH700829.3	SNOW	RC00
27	0.4879	0.0145	stkr	98	ASHTECH Z-XII3	ASH700718B		1L00-1D04
28	0.4850	0.0965	pot3	107	ASHTECH Z-XII3	ASH700829.3	SNOW	RC00
29	0.4837	0.0477	mlf1	112	ASHTECH Z-XII3	ASH700829.3	SNOW	RC00
30	0.4836	0.0520	ais1	107	ASHTECH Z-XII3	ASH700829.3	SNOW	RC00

Fig. 6
Average MP2 RMS values using 60° elevation mask. *Insert* shows the 30 most affected sites

Fig. 7
Stations CHA1 and CHA2 in Charleston, South Carolina

Fig. 9
Stations RED1 and RED2 in Reedy Point, Delaware

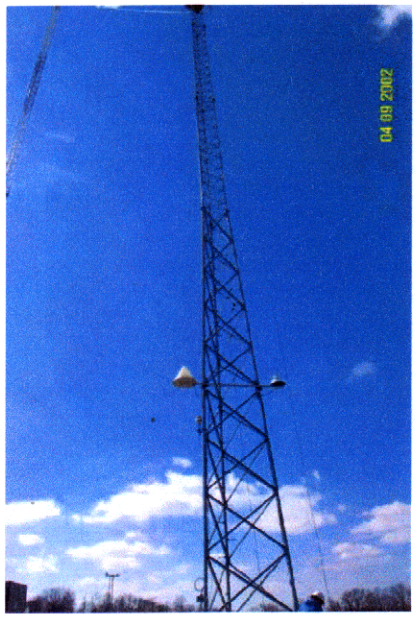

Fig. 8
Stations RIS1 and RIS2 in Rock Island, Iowa

Fig. 10
Stations LOU1 and LOU2 in Louisville, Kentucky

where $B_2 \equiv -\left(\frac{2\alpha}{\alpha-1}\right)n_1\lambda_1 + \left(\frac{2\alpha}{\alpha-1} - 1\right)n_2\lambda_2$.
In Eqs. (1) and (2) P_1 and P_2 represent the dual-frequency pseudorange observations, L_1 and L_2 represent the dual-frequency carrier phase observations, and m_1 and m_2 represent the dual-frequency carrier phase multipath. The MP1 and MP2 quantities vary in time mostly due to M_i and B_i, where M_i is the pseudorange multipath for frequency i=1, 2 and B_i is a bias related to the L1 and L2 integer carrier phase ambiguities, n_1 and n_2 . TEQC carefully monitors cycle slips and their effect on the bias terms B_i. In practice, the constant part of MP1 and MP2 (which for 30-s data is the average over the previous 50 epochs) is removed so what TEQC actually reports is the root mean square (RMS) variation of MP1 and MP2 for each satellite, as well as a mean RMS for all satellites. In MP1 and MP2, there remains the effects of pseudorange noise (<50 cm), carrier phase multipath (<7 cm), and carrier phase noise (<2 mm) but these are much smaller in size compared to the pseudorange multipath (which can be as large as 10 to 15 m at low elevation angles). Receivers such as the Ashtech Z-12, the Ashtech UZ-12, and the Allen Osborne

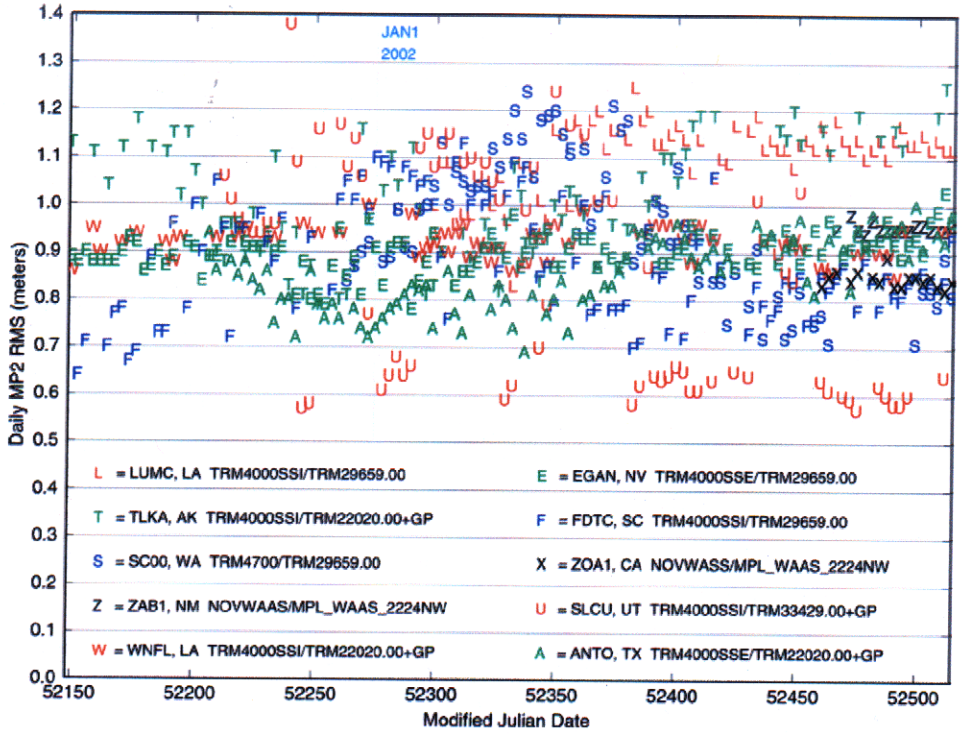

Fig. 11
Daily MP2 values for 10 selected sites from Fig. 4

Fig. 12
WAAS antenna housing used during 2002

Fig. 13
Station ANTO in San Antonio, Texas

ACT-family of receivers, collect three types of pseudo-ranges: C1 (C/A code), P1 (P-code), and P2 (P-code). When computing MP1, TEQC selects the more accurate P1 observable over the C1 observable. In a few instances, if P1 is unavailable in a RINEX file at a certain epoch then TEQC will use C1 instead. C1 is more affected by multipath than P1. If TEQC had been forced to use only the C1 observable (by removing all P1 observations from certain RINEX files) then the MP1 RMS values reported here for those 190 or so receivers that collect both C1 and P1 would have been significantly larger (e.g., the daily RMS values for the DGPS/NDGPS sites would have been increased by about 10 to 40%).

Description of the study

The TEQC software was run using RINEX files, each spanning 24 h with a 30-s sampling rate, for 390+ stations

Fig. 14
Stations YOU1 and YOU2 in Youngstown, New York

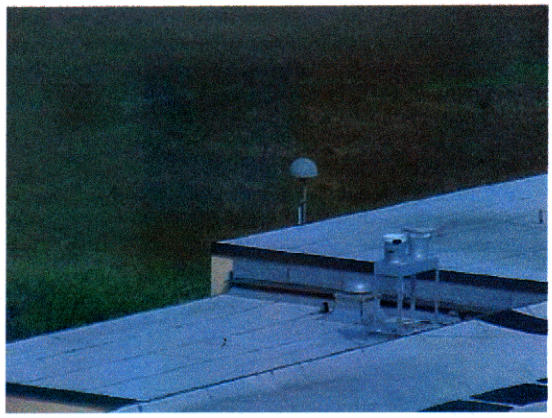

Fig. 15
Station LUMC in Lumcon, Louisiana

Fig. 16
Station FDTC in Florence, South Carolina

Fig. 17
Station GNAA in Glennallen, Alaska

from day 240, 2001, to day 240, 2002. Every third day was used for a total of about 120 days. For each day and each station, TEQC was run three times, using elevation mask angles of 10, 20, and 60°. The overall RMS for MP1 and MP2 from each run was included only if the site had at least 22 h of data with 90% of the data available. If an antenna or receiver was replaced at a site, then the site was afterwards counted as a new station. If a station had fewer than three acceptable days, it was ignored (this 3-day threshold was kept small for the sake of new stations recently added to the network). These daily RMS values were then combined into a yearly mean RMS for each station, and the associated sample standard deviations were computed. The yearly mean RMS values were computed for MP1 and MP2 for each of the three elevation mask angles. This was done to show which stations might be more affected by low-elevation-angle reflectors and which stations might be more affected by high-elevation-angle reflectors. The yearly mean RMS values and the sample standard deviations for all 390+ sites are shown plotted highest to lowest (most affected to least affected) in Figs. 1, 2, 3, 4, 5, 6. The 30 most affected sites are also listed in each figure along with their receiver type, antenna type, and firmware version. Since GPS users often use elevation cutoff angles of 15 or 20° when processing data, we expect that most readers will find the 20° elevation mask results the most interesting.

In the list of the most affected sites in Fig. 3, one can see that there are several maritime Differential GPS and Nationwide Differential GPS (DPGS/NDGPS) sites with a very large MP1 RMS values (these sites are the ones labeled as using ASHTECH Z-XII3 receivers and ASH700829.3 SNOW antennas). These same sites are present in Figs. 5 and 6, which indicates that they are being affected by high-elevation-angle multipath. This is most likely due to transmission towers located nearby which are used to broadcast correctors to Differential GPS (DGPS) users (Wolfe et al. 2000). The photographs in Figs. 7, 8, and 9 show some examples of these towers. To further verify that high-elevation-angle multipath was occurring, we plotted the epoch-by-epoch variation of

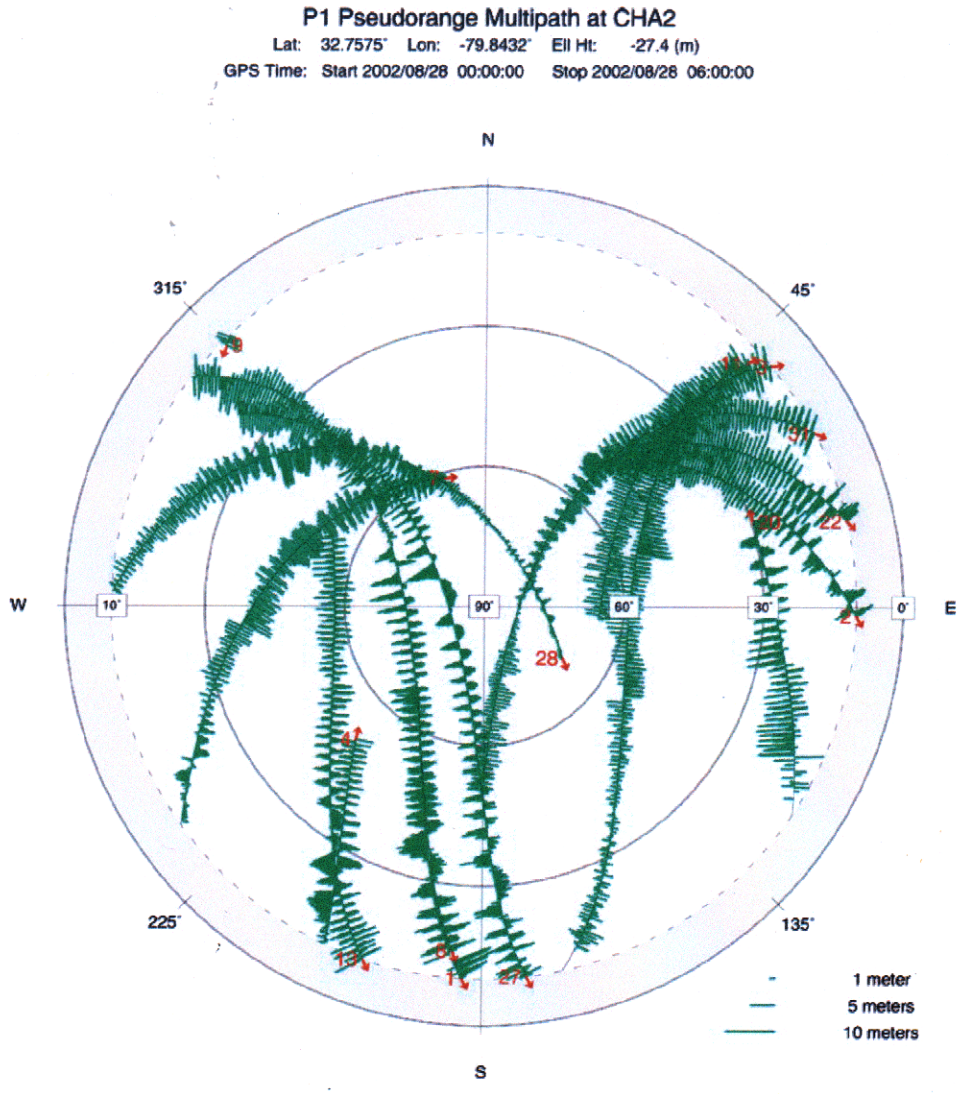

Fig. 18
MP1 values for station CHA2, using six hours of data

MP1 and MP2 for several of these stations using skyplots. Figures 18 and 19 show an example for station CHA2; skyplots for other DPGS/NDGPS stations such as RIS2 and RED1 showed similar high-elevation-angle multipath. In contrast, Figs. 20 and 21 show the MP1 and MP2 skyplots for one of the least affected stations in the CORS network, OKEE. Figures 18 and 19 clearly show that the severely affected DPGS/NDGPS sites seem to be much more affected in MP1 than MP2 (these figures were created using the P1 and P2 observables, respectively). Again, if Fig. 18 had been computed using the C1 observable instead of P1, the average magnitude of the MP1 multipath variations would have been about 40% larger. These skyplots were created using the epoch-by-epoch multipath variations found in the *.mp1 and *.mp2 plot files output by TEQC.

The list in Fig. 4 shows that for MP2, the 30 most affected stations now include many non- DPGS/NDGPS sites. A few of these sites are pictured in Figs. 13, 14, 15 ,16, 17; one can see that these photographs show no evidence of major reflectors. Figure 12 shows a picture of the WAAS antenna housing used at stations ZAB1, ZAB2, ZOA1, ZOA2, and ZJX1 during this study (the antenna elements were later replaced by the Federal Aviation Administration during the summer of 2003). Figure 11 shows the MP2 day-to-day variation for some of these non-DPGS/NDGPS sites. The beginning of 2002 is marked by the light blue line at Modified Julian Date (MJD) 52275.

Figure 22a, b plot the yearly mean MP1 RMS values versus the yearly mean MP2 RMS values for the 20° elevation mask. These figures show the yearly mean values for those sites which use the 12 most common receiver/antenna combinations in the network. In the legend in Fig. 22a, the numbers in parentheses represent the number of sites in the network that use each particular receiver/antenna combination. Table 1 and Table 2 show the 40 least affected sites for the 20° elevation mask, for MP1 and MP2, respectively. For the sake of brevity, we have shown only the 30 most affected sites (for all three mask angles) and the 40 least affected sites (for the 20°mask angle). A

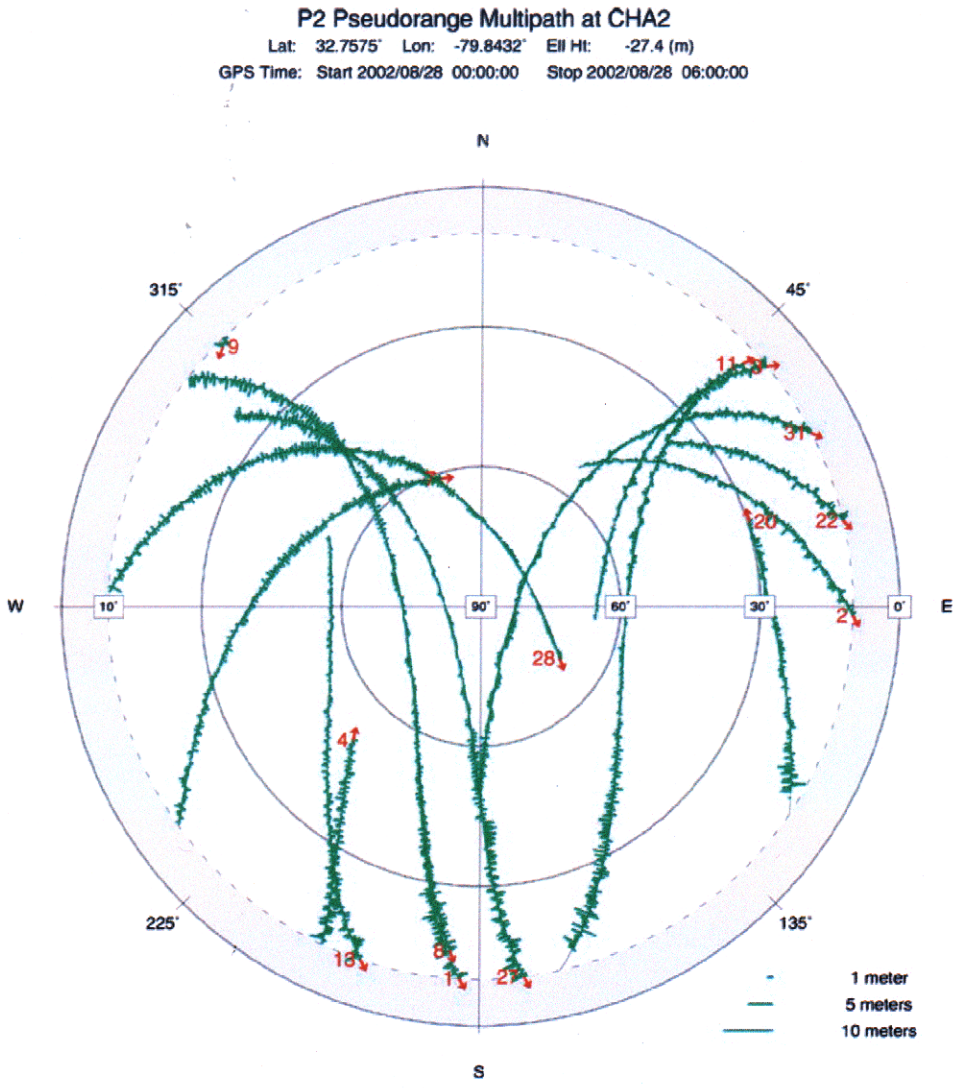

Fig. 19
MP2 values for station CHA2, using six hours of data

complete list of all 390+ sites, for MP1 and MP2, and for all three elevation masks, will be published in a later report.

Results

The lists in Figs. 5 and 6 show that the DPGS/NDGPS sites (those sites that use the ASHTECH Z-XII3 receiver and ASH700829.3 SNOW antenna) are most affected by high-elevation-angle reflectors. Figures 7, 8, 9 show photographs of some of these severely affected sites. As shown by Figs. 18 and 19, these high-reflector sites tend to be much more affected in MP1 than in MP2. However, the least affected DPGS/NDGPS sites in the network do not exhibit this interesting behavior, as shown in Fig. 22b by the Z symbols in the lower left corner. Although they are not shown in Tables 1 and 2, we noticed that the stations recently installed in Myton, Utah, and Pueblo, Colorado (which use pillars and choke ring antennas) are now among the best DGPS/NDGPS sites. Figures 3, 4, 5, and 6 show that two DGPS/NDGPS stations, LOU2 and YOU2, exhibit much larger MP1 and MP2 numbers than any other DPGS/NDGPS site. Station LOU2 as shown in Fig. 10 is mostly in the clear, its transmission tower is located about 150 ft to the west. The picture of YOU2 in Fig. 14 likewise seems to have no major obstructions or reflectors nearby. Because these two stations are so much worse than any other DPGS/NDGPS site, we expect that perhaps equipment problems are to blame (YOU2 was recently diagnosed as having had an antenna cable problem). Figures 3 and 4 show that their companion stations, YOU1 and LOU1, have high MP1 values but are not much affected in MP2.

Figure 4 shows that for MP2, the non-DPGS/NDGPS sites have the largest RMS values. Stations LUMC and COCD are actually the same station (station COCD was renamed to LUMC). This station is shown in Fig. 15. It is interesting to note that the Trimble receivers in the Fig. 4 list are accompanied by a mixture of choke ring antennas and

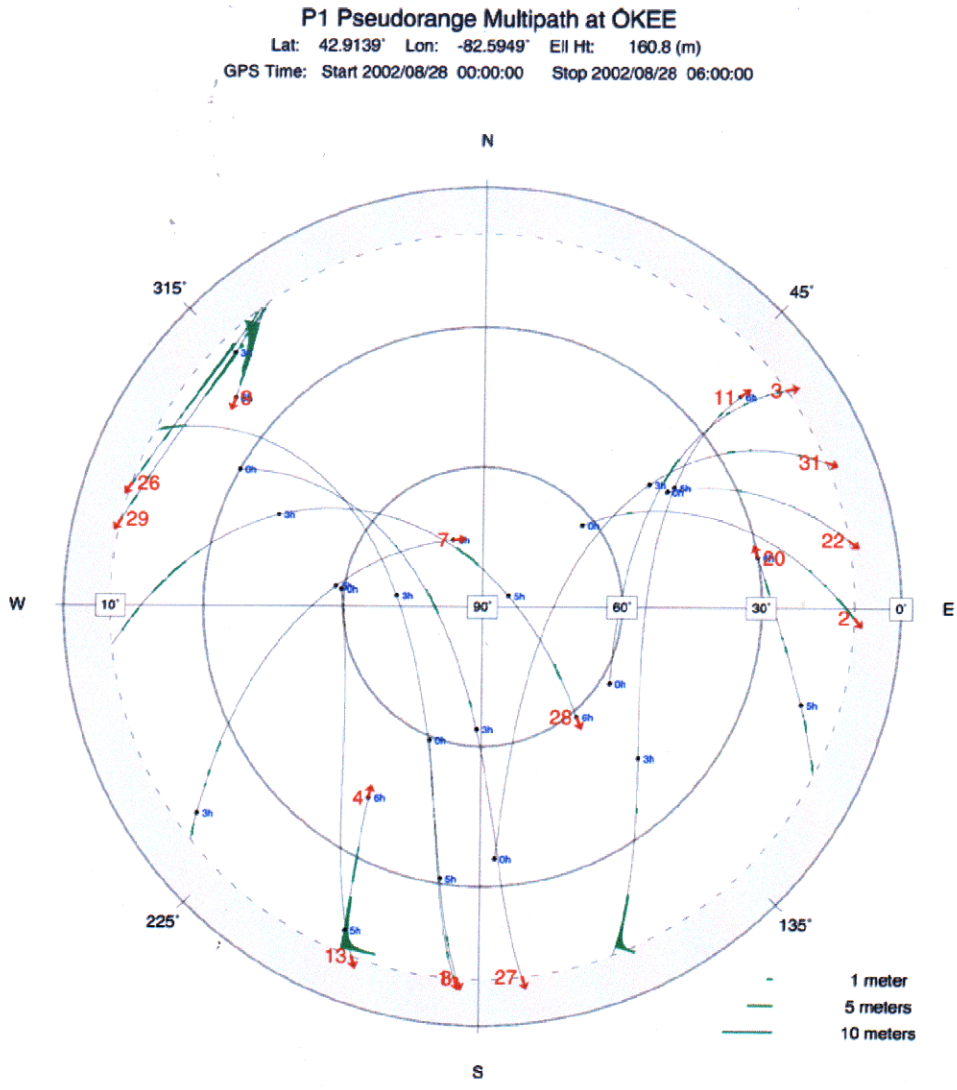

Fig. 20
MP1 values for station OKEE, using six hours of data

ground plane antennas. Figure 11 shows the variation of the daily MP2 values for 10 of these highly affected non-DPGS/NDGPS stations. Station SLCU (U) seems to have some very dramatic day-to-day variations, while the WAAS stations ZAB1 (Z) and ZOA1 (X) show very little deviation from one day to the next. In Fig. 11, the grouping of some days in a systematic manner may be related to temperature variations and/or precipitation at a site. Photographs of a few of these non-DPGS/NDGPS sites (ANTO, LUMC, FDTC, and GNAA) are shown in Figs. 13, 15, 16, 17.

Figures 18, 19, 20, 21 show examples of the range of multipath errors that can be found in the network. Station CHA2 is one of the most severely affected stations, and OKEE is one of the least affected. Looking closely at the photograph in Fig. 7 for stations CHA1 and CHA2 one can see that the transmission tower has been placed midway between the two GPS antennas. Station CHA2 is on the left and probably receives reflections from both the transmission tower (which rises up to a 75° angle when viewed from CHA2) and from the lighthouse in the background. It is interesting to note in Fig. 18 how large (5–6 m) the MP1 variations become, even above a 60° elevation angle (note that Fig. 18 was computed using only the P1 observable). These skyplots have proven to be a very useful tool for investigating individual sites.

Like Figs. 18 and 19, Fig. 22a shows how much more MP1 is affected versus MP2 for the severely affected DPGS/NDGPS sites. Figure 22b is a very interesting plot in that it shows how the newer receiver technology (such as the Ashtech UZ-12, Leica RS500, and Trimble 5700) has dramatically decreased the amounts of pseudorange multipath. It also shows how several of the DGPS/NDGPS sites and all of the WAAS sites seem to be among those most affected by pseudorange multipath (as mentioned above, the Federal Aviation Administration has since upgraded the antennas at all WAAS sites). It is also interesting to note how the older generation Trimble receivers seem to

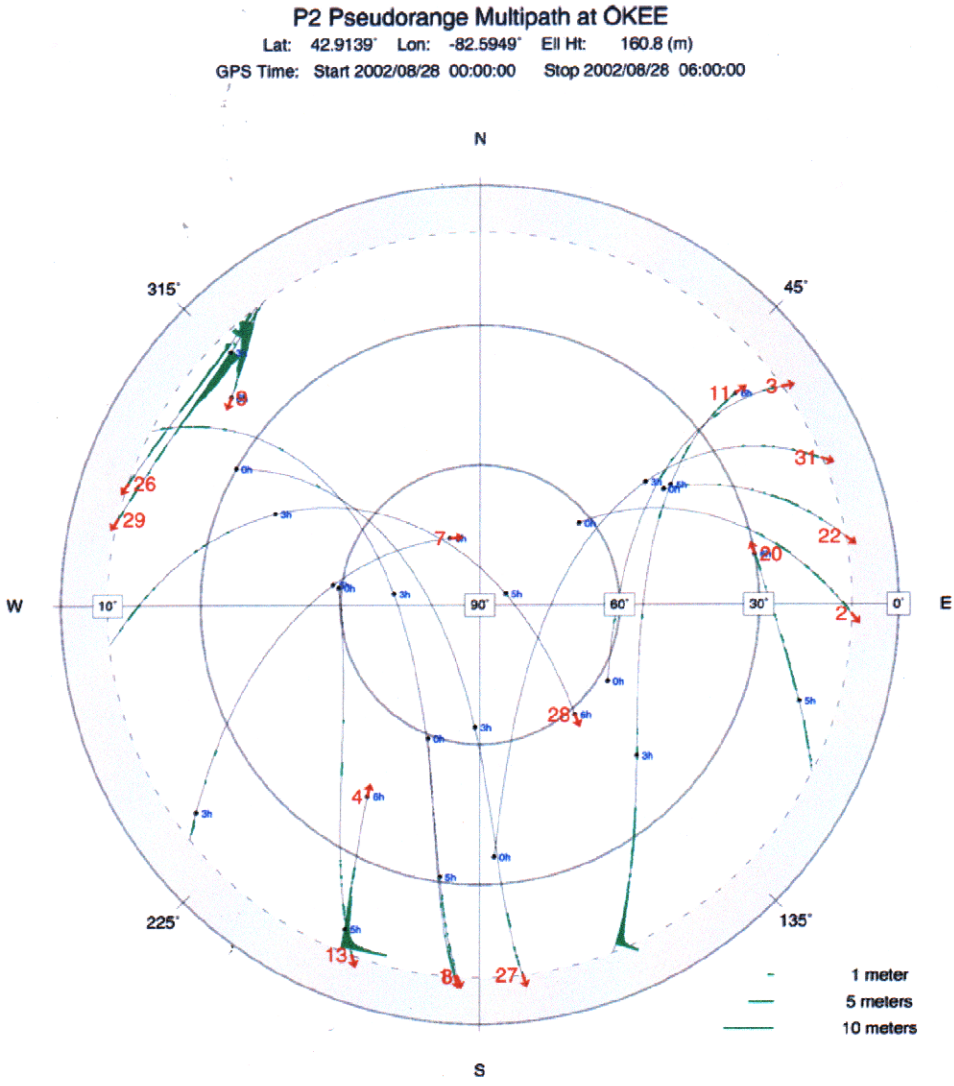

Fig. 21
MP2 values for station OKEE, using six hours of data

be much more affected in MP2 than MP1. The reader needs to keep in mind, however, that this figure does not take into account the differences in the multipath environment at the sites. It is possible that a well-performing receiver/antenna could have been consistently deployed at very poor site locations, and vice-versa. The reader should also keep in mind that newer receivers that do a good job mitigating pseudorange multipath may not necessarily improve the carrier phase multipath.

Tables 1 and 2 list the 40 least affected sites in the CORS network, for MP1 and MP2, respectively (using the 20°elevation mask). They are listed in order from worst to best (most affected to least affected). The Leica RS500 receivers from the state network in Michigan occupy the last 16 lines in Table 1. In Table 2, above the Leica RS500 sites, are several sites from the state network in Ohio which use the Trimble 5700 receiver and the TRM29659.00 antenna. For antenna mounts, these Ohio sites used very stable concrete pillars that extend about 10 ft below the ground and 8 ft above the ground. Figures 23 and 24 show examples of the Michigan and Ohio antenna mounts. Table 2 also lists several other good sites such as TSEA (Alaska), MINS (California), PUC1 (Utah), JAMA (Jamaica), UIUC (Illinois), and ATL1 (Georgia), which use various different receiver/antenna combinations to achieve excellent results.

Summary

This initial study has identified several DGPS/NDGPS sites that are severely affected by pseudorange multipath. Figures 18 and 19 show how examining the variation of MP1 and MP2 with respect to satellite azimuth and elevation can help to detect pseudorange multipath problems at high elevation angles. Photographs obtained for this study clearly show how some sites can become problematic when GPS antennas are placed in close proximity to transmission towers and other types of navigational aides. While

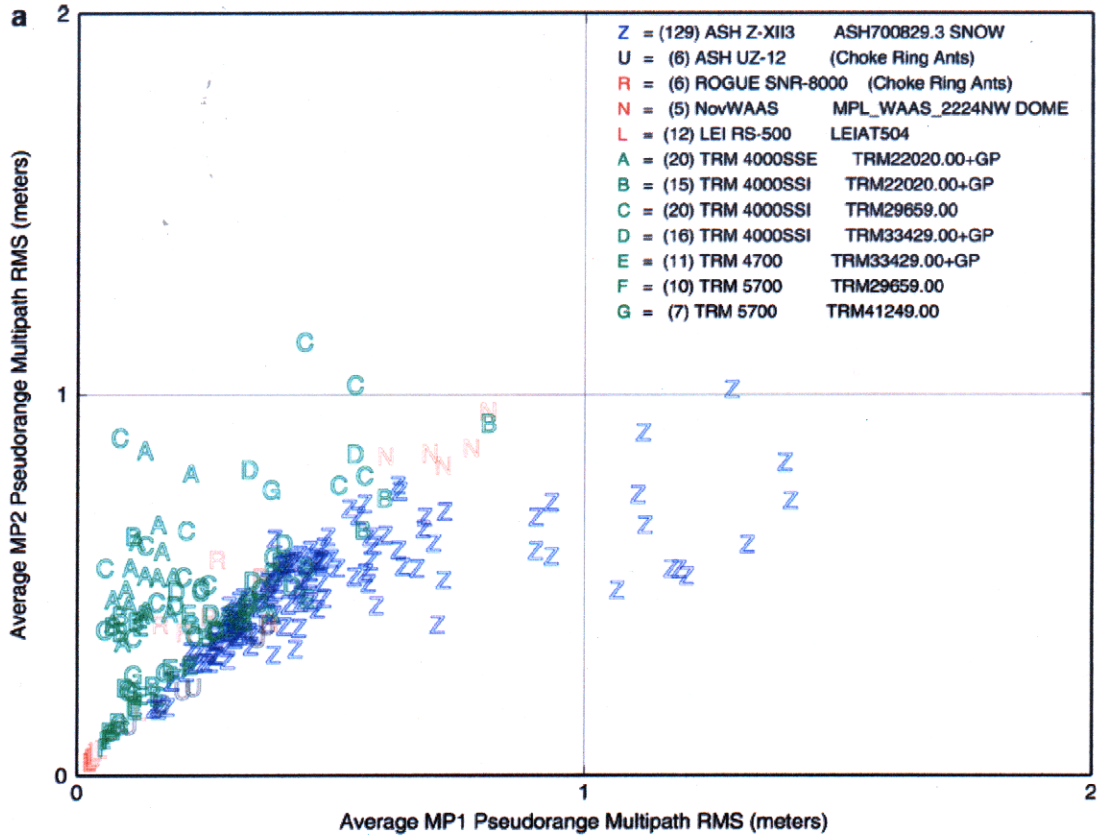
a
Z = (129) ASH Z-XII3 ASH700829.3 SNOW
U = (6) ASH UZ-12 (Choke Ring Ants)
R = (6) ROGUE SNR-8000 (Choke Ring Ants)
N = (5) NovWAAS MPL_WAAS_2224NW DOME
L = (12) LEI RS-500 LEIAT504
A = (20) TRM 4000SSE TRM22020.00+GP
B = (15) TRM 4000SSI TRM22020.00+GP
C = (20) TRM 4000SSI TRM29659.00
D = (16) TRM 4000SSI TRM33429.00+GP
E = (11) TRM 4700 TRM33429.00+GP
F = (10) TRM 5700 TRM29659.00
G = (7) TRM 5700 TRM41249.00
Average MP2 Pseudorange Multipath RMS (meters)
Average MP1 Pseudorange Multipath RMS (meters)
0
1
2

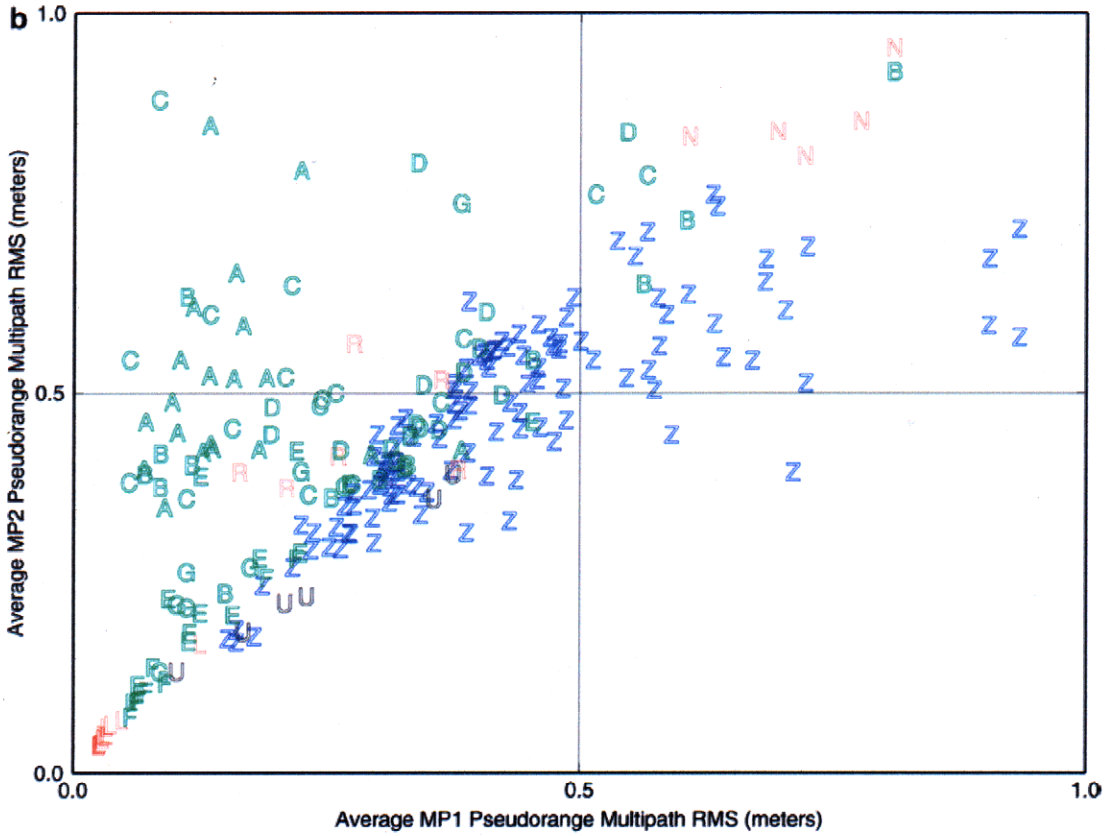
b
Average MP2 Pseudorange Multipath RMS (meters)
Average MP1 Pseudorange Multipath RMS (meters)
0.0
0.5
1.0

Table 1
Average MP1 RMS for one year using a 20° Elev. Mask (40 least affected sites listed highest to lowest)

Rank	MP1	Std dev	Site	# of days	Receiver type	Antenna type	Firmware
362	0.0859	0.0207	wil1	113	TRIMBLE 4000SSI	TR-M22020.00+GP	7.29
363	0.0855	0.0279	pit1	109	TRIMBLE 4000SSI	TR-M22020.00+GP	7.29
364	0.0853	0.0164	bsmk	43	TRIMBLE 5700	TRM41249.00	1.04
365	0.0813	0.0140	fdtc	106	TRIMBLE 4000SSI	TRM29659.00	7.32
366	0.0795	0.0069	bsmk	20	TRIMBLE 5700	TR-M33429.00+GP	1.04
367	0.0787	0.0043	ospa	30	TRIMBLE 5700	ASH701945B_-M	1.04
368	0.0781	0.0384	pktn	73	TRIMBLE 5700	TRM29659.00	1.04
369	0.0718	0.0549	mcon	74	TRIMBLE 5700	TRM29659.00	1.04
370	0.0711	0.0092	corc	87	TRIMBLE 4000SSE	TR-M22020.00+GP	7.29
371	0.0700	0.0153	stpl	18	TRIMBLE 4000SSI	TR-M22020.00+GP	7.29
372	0.0697	0.0281	arl5	92	TRIMBLE 4000SSE	TR-M22020.00+GP	7.29
373	0.0660	0.0500	sidn	72	TRIMBLE 5700	TRM29659.00	1.04
374	0.0650	0.0173	eprt	113	TRIMBLE 4000SSI	TRM29659.00 DOME	7.27
375	0.0649	0.0417	corb	104	TRIMBLE 4000SSI	AOAD/M_T	7.29
376	0.0642	0.0072	mins	90	ASHTECH Z-XII3	AOAD/M_T	1E95
377	0.0636	0.0171	gust	56	TRIMBLE 5700	TRM29659.00	1.04
378	0.0632	0.0063	puc1	110	TRIMBLE 4700	TR-M33429.20+GP	1.30
379	0.0627	0.0459	colb	60	TRIMBLE 5700	TRM29659.00	1.04
380	0.0601	0.0159	npri	107	TRIMBLE 4000SSI	TRM29659.00 DOME	7.29
381	0.0583	0.0077	freo	71	TRIMBLE 5700	TRM29659.00	1.04
382	0.0559	0.0202	leba	74	TRIMBLE 5700	TRM29659.00	1.04
383	0.0556	0.0053	adks	9	TRIMBLE 4000SSI	TRM29659.00	7.22
384	0.0550	0.0055	adks	6	TRIMBLE 4000SSI	TRM29659.00 TCWD	7.22
385	0.0547	0.0290	s300	109	TRIMBLE 4000SSI	TRM29659.00	7.29
386	0.0478	0.0238	nor2	58	LEICA RS500	LEIAT504 LEIS	3.00
387	0.0425	0.0158	adri	60	LEICA RS500	LEIAT504 LEIS	3.00
388	0.0368	0.0095	sup1	57	LEICA RS500	LEIAT504 LEIS	3.00
389	0.0354	0.0095	siby	26	LEICA RS500	LEIAT504 LEIS	3.00
390	0.0335	0.0094	grar	68	LEICA RS500	LEIAT504 LEIS	3.00
391	0.0331	0.0176	brig	77	LEICA RS500	LEIAT504 LEIS	3.00
392	0.0313	0.0141	sup2	54	LEICA RS500	LEIAT504 LEIS	3.00
393	0.0290	0.0071	sowr	59	LEICA RS500	LEIAT504 LEIS	3.00
394	0.0287	0.0079	mple	52	LEICA RS500	LEIAT504 LEIS	3.00
395	0.0287	0.0183	univ	54	LEICA RS500	LEIAT504 LEIS	3.00
396	0.0260	0.0193	metr	68	LEICA RS500	LEIAT504 LEIS	3.00
397	0.0250	0.0152	nor1	66	LEICA RS500	LEIAT504 LEIS	3.00
398	0.0247	0.0148	bayr	75	LEICA RS500	LEIAT504 LEIS	3.00
399	0.0247	0.0161	sup3	53	LEICA RS500	LEIAT504 LEIS	3.00
400	0.0233	0.0058	okee	21	LEICA RS500	LEIAT504 LEIS	3.00
401	0.0233	0.0074	lans	39	LEICA RS500	LEIAT504 LEIS	3.00

this kind of severe multipath can hinder precise kinematic applications using pseudoranges, it is important to remember that many static applications which collect data over longer time spans (one half hour or longer) can effectively average out the effects of multipath for pseudorange and carrier phase observations. The non-DGPS/NDGPS stations, which were affected mostly in MP2, do not appear to have any obstructions/reflectors nearby and hence are much more puzzling. We suspect that how the antennas are mounted can play a major role. We saw several stations with pseudorange multipath problems

◀

Fig. 22
a MP1 versus MP2 for the 12 most common receiver/antenna combinations. b MP1 versus MP2 (enlarged to show detail)

Table 2
Average MP2 RMS for one year using a 20° Elev. Mask (40 least affected sites listed highest to lowest)

Rank	MP2	Std dev	Site	# of days	Receiver type	Antenna type	Firmware
362	0.1686	0.0648	nor3	59	LEICA RS500	LEIAT504 LEIS	3.00
363	0.1655	0.0359	elen	77	TRIMBLE 4000SSE	TRM29659.00 UNAV	7.29
364	0.1625	0.0095	chab	115	ASHTECH Z-XII3	ASH700936A_-M	CB00
365	0.1624	0.0116	cndr	80	ASHTECH Z-XII3	ASH700936D_-M	CB00
366	0.1516	0.0064	amc2	96	AOA SNR-12 ACT	AOAD/M_T	3.3.32.4
367	0.1508	0.0184	fair	92	AOA SNR-8100 ACT	JPL D/M+CRT	3.3.32.2
368	0.1494	0.1119	cnmi	110	TRIMBLE 4700	TR-M33429.20+GP DOME	7.29
369	0.1471	0.0049	atl1	7	LEICA SR9500	LEIAT303	
370	0.1384	0.0487	pktn	73	TRIMBLE 5700	TRM29659.00	
371	0.1379	0.0077	uiuc	34	TRIMBLE 4700	TR-M33429.00+GP	
372	0.1323	0.0180	bsmk	43	TRIMBLE 5700	TRM41249.00	1.04
373	0.1322	0.0283	jama	79	ASHTECH UZ-12	AOAD/M_TA_NGS	UG00
374	0.1210	0.0091	bsmk	20	TRIMBLE 5700	TR-M33429.00+GP	1.04
375	0.1174	0.0558	woos	72	TRIMBLE 5700	TRM29659.00	1.04
376	0.1151	0.0067	puc1	110	TRIMBLE 4700	TR-M33429.20+GP	1.30
377	0.1130	0.0053	ospa	30	TRIMBLE 5700	ASH701945B_-M	1.04
378	0.1068	0.0618	mcon	74	TRIMBLE 5700	TRM29659.00	1.04
379	0.1058	0.0612	sidn	72	TRIMBLE 5700	TRM29659.00	1.04
380	0.0940	0.0643	colb	60	TRIMBLE 5700	TRM29659.00	1.04
381	0.0936	0.0208	gust	56	TRIMBLE 5700	TRM29659.00	1.04
382	0.0920	0.0104	freo	71	TRIMBLE 5700	TRM29659.00	1.04
383	0.0850	0.0113	mins	90	ASHTECH Z-XII3	AOAD/M_T	1E95
384	0.0781	0.0133	siby	26	LEICA RS500	LEIAT504 LEIS	3.00
385	0.0750	0.0194	adri	60	LEICA RS500	LEIAT504 LEIS	3.00
386	0.0745	0.0164	tsea	67	LEICA CRS1000	LEIAT504	5.16
387	0.0730	0.0251	leba	74	TRIMBLE 5700	TRM29659.00	1.04
388	0.0688	0.0287	nor2	58	LEICA RS500	LEIAT504 LEIS	3.00
389	0.0632	0.0104	sup1	57	LEICA RS500	LEIAT504 LEIS	3.00
390	0.0600	0.0236	brig	77	LEICA RS500	LEIAT504 LEIS	3.00
391	0.0573	0.0105	mple	52	LEICA RS500	LEIAT504 LEIS	3.00
392	0.0493	0.0108	sowr	59	LEICA RS500	LEIAT504 LEIS	3.00
393	0.0491	0.0136	sup2	54	LEICA RS500	LEIAT504 LEIS	3.00
394	0.0490	0.0098	grar	68	LEICA RS500	LEIAT504 LEIS	3.00
395	0.0446	0.0206	univ	54	LEICA RS500	LEIAT504 LEIS	3.00
396	0.0381	0.0235	metr	68	LEICA RS500	LEIAT504 LEIS	3.00
397	0.0368	0.0121	sup3	53	LEICA RS500	LEIAT504 LEIS	3.00
398	0.0365	0.0176	nor1	66	LEICA RS500	LEIAT504 LEIS	3.00
399	0.0356	0.0099	lans	39	LEICA RS500	LEIAT504 LEIS	3.00
400	0.0345	0.0172	bayr	75	LEICA RS500	LEIAT504 LEIS	3.00
401	0.0338	0.0080	okee	21	LEICA RS500	LEIAT504 LEIS	3.00

even though they were using choke ring antennas and had no above-horizon reflectors. More work needs to be done to quantify the effects of mounting various types of choke ring antennas on pipes, metal stands, and threaded rods. The study has also pointed out success stories: those networks in Ohio and Michigan where a combination of new receiver/antenna technology, excellent antenna mounting, and good site location has dramatically lowered the effects of pseudorange multipath. The comparison of different receiver/antenna combinations shown in Fig. 22b would seem to indicate that for several manufacturers the newer generation receivers do a much better job of mitigating pseudorange multipath than their predecessors. It is important to note that if the pseudorange data used by TEQC has been smoothed, then the MP1 and MP2 numbers tend to look overly optimistic. Thus, we insured that the Ashtech Z-XII3 and Ashtech UZ-12 RINEX files were created with the pseudorange smoothing option in TEQC

Fig. 23
Station METR in the Michigan Network

Fig. 24
Station COLB in the Ohio Network

turned off. At the time, these were the only receiver types included in this study whose raw data format allowed for this option. The existence of high-elevation-angle reflectors at some DGPS/NDGPS sites would make it difficult to use carrier phase calibration techniques such as those described by Wanninger and May (2001) for the National CORS Network. However, with knowledge of which sites are severely affected by multipath, one can experiment with other in-situ carrier phase calibration techniques to see how well they perform at these very challenging sites.

Acknowledgements The photographs for stations CHA1, CHA2, and FDTC in South Carolina were supplied by Lewis Lapine and Dick Woods of the South Carolina Geodetic Survey. The photographs for stations LOU1 and LOU2 in Kentucky were supplied by Ross MacKay, the NGS State Advisor for Kentucky. The photographs for stations YOU1 and YOU2 in New York were supplied by David Conner, the NGS State Advisor for Ohio. The photographs for stations RED1 and RED2 in Delaware were supplied by Mr. Ed Berchtold. The photographs of stations RIS1 and RIS2 in Iowa were supplied by Mr. Charles Smith of the U.S. Coast Guard. All other photographs of individual sites were taken from the NGS CORS Website http://www.ngs.noaa.gov/CORS.

References

Brown A, Wang J (1999) High accuracy kinematic GPS performance using a digital beam-steering array. In: Proceedings of ION GPS-99, Nashville, Tennessee, September 14–17, pp 1685–1693

Estey LH, Meertens CM (1999) TEQC: the multi-purpose toolkit for GPS/GLONASS data. GPS Solutions (3)1:42–49

Wanninger L, May M (2001) Carrier-phase multipath calibration of GPS reference stations. J Inst Navigation, (48)2:113–124

Wolfe DB, Judy CL, Haukkala EJ, Godfrey DJ (2000) Implementing and engineering an NDGPS network in the United States. In: Proceedings of ION 2000, Salt Lake City, Utah, September 19–22, pp 1254-1263